$CD8^+\alpha\beta^+$ T Cells That Lack Surface CD5 Antigen Expression Are a Major Lymphotactin (XCL1) Source in Peripheral Blood Lymphocytes

Laura Stievano, Valeria Tosello, Novella Marcato, Antonio Rosato, Annalisa Sebelin, Luigi Chieco-Bianchi and Alberto Amadori

J Immunol 2003;171;4528-4538

The Journal of Immunology is published twice each month by The American Association of Immunologists, Inc., 9650 Rockville Pike, Bethesda, MD 20814-3994.

Print ISSN: 0022-1767 Online ISSN: 1550-6606.

$CD8^+\alpha\beta^+$ T Cells That Lack Surface CD5 Antigen Expression Are a Major Lymphotactin (XCL1) Source in Peripheral Blood Lymphocytes[1]

Laura Stievano, Valeria Tosello, Novella Marcato, Antonio Rosato, Annalisa Sebelin, Luigi Chieco-Bianchi, and Alberto Amadori[2]

To better characterize the cellular source of lymphotactin (XCL1), we compared XCL1 expression in different lymphocyte subsets by real-time PCR. XCL1 was constitutively expressed in both PBMC and $CD4^+$ cells, but its expression was almost 2 log higher in $CD8^+$ cells. In vitro activation was associated with a substantial increase in XCL1 expression in both PBMC and $CD8^+$ cells, but not in $CD4^+$ lymphocytes. The preferential expression of XCL1 in $CD8^+$ cells was confirmed by measuring XCL1 production in culture supernatants, and a good correlation was found between figures obtained by real-time PCR and XCL1 contents. XCL1 expression was mostly confined to a $CD3^+CD8^+$ subset not expressing CD5, where XCL1 expression equaled that shown by $\gamma\delta^+$ T cells. Compared with the $CD5^+$ counterpart, $CD3^+CD8^+CD5^-$ cells, which did not express CD5 following in vitro activation, showed preferential expression of the $\alpha\alpha$ form of CD8 and a lower expression of molecules associated with a noncommitted/naive phenotype, such as CD62L. $CD3^+CD8^+CD5^-$ cells also expressed higher levels of the XCL1 receptor; in addition, although not differing from $CD3^+CD8^+CD5^+$ cells in terms of the expression of most α- and β-chemokines, they showed higher expression of CCL3/macrophage inflammatory protein-1α. These data show that TCR $\alpha\beta$-expressing lymphocytes that lack CD5 expression are a major XCL1 source, and that the contribution to its synthesis by different TCR $\alpha\beta$-expressing T cell subsets, namely $CD4^+$ lymphocytes, is negligible. In addition, they point to the $CD3^+CD8^+CD5^-$ population as a particular T cell subset within the $CD8^+$ compartment, whose functional properties deserve further attention. ***The Journal of Immunology*****, 2003, 171: 4528–4538.**

The chemokines are a large family of cytokines whose primary biologic function is to control the trafficking of various leukocyte populations through different lymphoid compartments and sites of inflammation (1, 2). Based on the number and position of conserved cysteine residues, four subfamilies can be identified (3, 4), designated CXC (α-chemokines), CC (β-chemokines), C (γ-chemokines), and CX_3C (δ-chemokines). Whereas the CXC and CC families comprise an increasingly growing number of members, only two and one representative have been as yet identified for the γ and δ families, respectively. CXC chemokines mainly target neutrophils and T cells, whereas CC chemokines mostly act on monocytes, eosinophils, basophils, and T cells (5); both families play a relevant role in several leukocyte functions, including migration, proliferation, cytotoxicity, adhesion, and apoptosis (5, 6). Until a few years ago, the only known role for the δ-chemokine fractalkin and the γ-chemokine lymphotactin (XCL1)[3] was the ability to promote migration of different leukocyte subpopulations. In particular, XCL1 is efficiently chemotactic for activated $CD4^+$ and $CD8^+$ T cells and NK cells (7–9); more recently, a chemotactic activity on neutrophils and B cells was also demonstrated (10).

A renewed interest in the possible functions of XCL1 other than promotion of leukocyte migration has recently arisen. Two major problems remain, however, and deserve more attention. First, the source of XCL1 within the immune system is still poorly defined. On the one hand, lymphotactin synthesis was originally described as strictly confined to $CD8^+$ T cells (8–12); more recently, XCL1 expression was also reported in several other leukocyte populations, including NK cells (7, 13, 14), dendritic cells (15), activated mast cells (16), TCR $\gamma\delta^+$ T cells (17, 18), and even $CD4^+$ T cells (19), especially those belonging to the Th1 subset (20, 21). In most cases, however, no quantitative comparisons between different cell populations were performed, and the ability to produce XCL1 was mostly evaluated by nonquantitative PCR approaches. Second, the role of lymphotactin in regulating T cell function is debated. On the one hand, XCL1 seems to impair Th1 function in humans (22); on the other, it seems to favor cellular responses (23, 24) and to promote antitumor activity through adjuvant-like properties in murine models (25–29).

In view of these observations, we decided to address the first issue and to better characterize the lymphotactin cellular source(s) by comparing XCL1 expression by quantitative real-time PCR assay and ELISA in different lymphocyte populations. Here we show that in humans XCL1 expression is mainly a property of $CD8^+$ T cells, and that the contribution to its synthesis by different TCR $\alpha\beta$-expressing T cell subsets, namely $CD4^+$ lymphocytes, is negligible. Within the $CD8^+$ population, the major contribution is from a subset lacking CD5 Ag expression, which also shows several peculiar

Department of Oncology and Surgical Sciences, University of Padova, Padova, Italy

Received for publication January 27, 2003. Accepted for publication August 14, 2003.

The costs of publication of this article were defrayed in part by the payment of page charges. This article must therefore be hereby marked *advertisement* in accordance with 18 U.S.C. Section 1734 solely to indicate this fact.

[1] This work was supported in part by grants from Ministry of Health (ISS, AIDS Project), Italian Association for Research on Cancer, Italian Federation for Research on Cancer, and MIUR 60% and 40%.

[2] Address correspondence and reprint requests to Dr. Alberto Amadori, Department of Oncology and Surgical Sciences, University of Padova, Via Gattamelata 64, I-35128 Padova, Italy. E-mail address: albido@unipd.it

[3] Abbreviations used in this paper: XCL1, lymphotactin; Ct, threshold cycle; Rn, normalized reporter signal; SN, supernatant.

0022-1767/03/$02.00

phenotypic and functional properties compared with CD5-expressing, "orthodox" $CD8^+$ T cells.

Materials and Methods

Purification of T lymphocyte subsets

The blood samples employed in these studies were obtained from healthy adult donors (ages 20–47 years) after they gave their informed consent. PBMC were isolated from buffy coats by Ficoll-Hypaque (Pharmacia-Biotech, Uppsala, Sweden) gradient centrifugation (30) and resuspended in RPMI 1640 medium. Lymph node samples were obtained from patients undergoing minor surgery; histological examination of the tissue showed no gross abnormalities. Tonsils as well as blood samples were obtained from patients (ages 3–7 years) undergoing tonsillectomy. The tissues were minced with scissors to obtain single-cell suspensions, which were analyzed cytofluorometrically as detailed below.

$CD4^+$ and $CD8^+$ cells were obtained by positive selection on LS columns using the high gradient magnetic cell separation system MACS (Miltenyi Biotec, Bergish Gladbach, Germany) after incubation with anti-CD4 and anti-CD8 MicroBeads, according to the manufacturer's instructions. The purity of recovered cells was >98%, with no detectable cross-contamination by $CD8^+$ and $CD4^+$ cells, as determined by cytofluorometric analysis.

A more complex separation procedure was employed to obtain purified $CD8^+$ T cell subpopulations. To isolate $CD3^+CD8^+CD5^-$ cells, PBMC were first incubated with anti-CD5 mAb (clone CB01; courtesy of F. Malavasi, Turin, Italy) and then with goat anti-mouse IgG MicroBeads (Miltenyi Biotec). The labeled cells were subsequently passed through a CS column specific for negative selection; unlabeled cells ($CD5^-$ fraction) were incubated with anti-CD8 Multisort MicroBeads and processed according to the above positive selection protocol. After discarding the magnetic MicroBeads, the $CD5^-CD8^+$ T cell subset thus obtained underwent positive selection with anti-CD3 MicroBeads (Miltenyi Biotec). By the end of the fractionation procedures, >99% of the cells of the resulting population were viable and expressed CD5, CD8, and CD3.

To purify $CD3^+CD8^+CD5^+$ cells, a different separation protocol was adopted. $CD8^+$ cells were first isolated from PBMC using anti-CD8 Multisort MicroBeads; after removing magnetic beads according to the manufacturer's instructions, $CD5^-$ cells were depleted from the $CD8^+$ fraction with anti-CD5 mAb. Cytofluorometric analysis of the resulting cell population showed that >98% of the cells were $CD8^+CD5^+$ cells, 99% of which also expressed the CD3 marker.

In a set of experiments, TCR $\alpha\beta$- and TCR $\gamma\delta$-expressing T cells were isolated by positive selection with the relevant mAb (BD Biosciences, Heidelberg, Germany) and MicroBeads as described above; the purity of the recovered populations always exceeded 98%.

In vitro cell culture

Unfractionated PBMC, $CD4^+$ cells, $CD8^+$ cells, $CD3^+CD8^+CD5^-$, and $CD3^+CD8^+CD5^+$ cells were cultured at a concentration of 1×10^6/ml in RPMI medium supplemented with 10% FCS (Life Technologies, Gaithersburg, MD), 2×10^{-5} 2-ME, 100 μg/ml nonessential amino acids, and 100 μg/ml L-glutamine (complete RPMI). Each subpopulation was cultured alone and in the presence of the calcium ionophore A23187 (500 ng/ml) and PMA (1 ng/ml; both from Sigma-Aldrich, St. Louis, MO) for 4 h; a cell aliquot was also incubated for 30 h in 24-well plates precoated with anti-CD3 mAb (clone CBT-3; provided by F. Malavasi, Turin, Italy), as described previously (31). At the end of the stimulation period, culture supernatants (SN) were harvested and used for ELISA; the cells were instead pelleted and frozen for subsequent molecular analysis.

In a set of experiments, PBMC and purified $CD4^+$ or $CD8^+$ cells were activated with the anti-CD3 mAb as described above and cultured with rIL-2 (EuroCetus-Chiron, Milan, Italy; 50 U/ml, final concentration) in both the absence and the presence of an anti-CD28 mAb (Coulter-Immunotech, Marseilles, France; 10 μg/ml). Cell and SN samples were harvested after 24, 48, 96, and 168 h from culture initiation and were processed as described above for molecular and ELISA analyses.

RNA preparation

RNA was extracted from the different cell populations as reported previously (32) using the RNeasy Mini kit (Qiagen, Chatsworth, CA), according to the manufacturer's instructions. The final RNA pellet was dissolved in 30 μl of RNase-free water. RNA contents were determined spectrophotometrically, and 1 μg of RNA was used for reverse transcription. cDNA synthesis was performed in a total volume of 100 μl of RNase-free water, including 2.5 mM dNTPs, 50 μM random hexamers, 25 mM $MgCl_2$, 20 U/ml RNase inhibitor, and 125 U MultiScribe Reverse Transcriptase. All the above reagents were purchased from PerkinElmer (Emeryville, CA). Retrotranscription conditions were as follows: 30 min at 42°C, 5 min at 99°C, and 1 h at 4°C.

Nonquantitative PCR analysis of XCL1, XCR1, and CD5 expression

For XCL1 expression analysis, PCR was performed in a 50-μl volume containing 2 μl of the cDNA fragments, 0.2 U of AmpliTaq Gold polymerase (PerkinElmer), 200 μM dNTPs (Amersham Pharmacia Biotech, Arlington Heights, IL), GeneAmp 10× PCR Buffer II (PerkinElmer), 1.5 mM $MgCl_2$, and 25 pM XCL1-specific primers (forward, 5′-CGACCTCAGCCATGAGACTTC-3′; reverse, 5′-CTGCCAGAGACTACTAGCCAG-3′, corresponding to nt 5–25 and nt 351–371 in the cDNA sequence (accession no. U23772)). The PCR conditions were as follows: one cycle at 95°C for 10 min, followed by 30 cycles at 95°C for 30 s, 56°C for 30 s, 72°C for 1 min, and a final extension cycle at 72°C for 7 min. For the control of RNA and cDNA preparations, we used RT-PCR for β-actin (33). Amplified products were analyzed electrophoretically on 1.8% agarose gel and were visualized under UV rays after ethidium bromide staining.

For XCR1 expression detection, the primers (forward, 5′-ATGGAGTCCTCAGGCAACCC-3′; reverse, 5′-CAGGAAGAAGATGCTGCTGT-3′) were designed to generate a product of 360 nt (accession no. NM005283). The amplification profile was composed of denaturation at 94°C for 30 s, annealing at 57°C for 30 s, and extension at 72°C for 30 s. The 30 cycles were preceded by denaturation at 95°C for 5 min and were immediately followed by a final extension at 72°C for 7 min.

The primers used to amplify CD5 cDNA (forward, 5′-GGTATGACCCAGATTTCCAG-3′; reverse, 5′-AATGCTCCAGGGAGGTACAG-3′) were designed to encompass a region of 665 nt in the cDNA sequence (accession no. X89405); PCR was performed using the above conditions.

Real-time PCR analysis of XCL1 and XCR1

XCL1 expression was evaluated by a quantitative real-time PCR assay, based on the 5′-3′ exonuclease activity of the *Taq* DNA polymerase, as detailed previously (34). Primers and probes specific for the amplification of the human XCL1 and GAPDH genes were obtained from PE Applied Biosystems (Foster City, CA). PCR was performed in duplicate using a final concentration of 175 nM probe and 600 nM primers. The amplification process was conducted in an ABI/PRISM 7700 Sequence Detector System (PE Applied Biosystems) under the following conditions: an initial denaturation step (2 min at 95°C), followed by 45 cycles of 15 s at 95°C and 60 s at 60°C. For each reaction tube, the fluorescence signal of the reporter dye (FAM-6-carboxyfluorescein for XCL1 and VIC-β-glucuronidase for GAPDH) was divided by the fluorescence signal of the passive reference dye (TAMRA-6carboxy-tetramethyl-rhodamine) to obtain a reference defined as the normalized reporter signal (Rn). This system produced a real-time amplification plot based on normalized fluorescence signal; ΔRn, which represents the normalized reporter signal (Rn) minus the baseline signal established in the first 15 PCR cycles, increases during PCR as the XCL1 transcript increases, until the reaction reaches a plateau. The fractional cycle number at which the amount of amplified target reached a fixed threshold, called the threshold cycle (Ct), was determined. The Ct obtained was equivalent to the initial number of templates in the sample. To quantify XCL1 message in the different lymphocyte subsets, the Ct of each well was plotted against the reference curve, prepared by amplifying serial dilutions of cDNA derived from unfractionated PBMC, whose constitutive expression of XCL1 was known from literature (7, 12). To minimize the influence of DNA quality and to normalize the samples for cell equivalents, a second real-time PCR assay targeting the GAPDH gene was performed under the same PCR conditions. As performed for the XCL1 standard curve, a reference curve to quantify GAPDH was generated by amplifying serial dilutions of cDNA derived from PBMC. Appropriate negative controls (cDNA obtained from nonlymphoid cells, such as MCF7 and MDA cells, and distilled water) were included in each set of experiments.

Real-time PCR to detect XCL1 receptor gene (XCR1) expression was performed using the TaqMan assay essentially as described for XCL1. The oligonucleotide primers and the fluorogenic probe specific for XCR1 were as follows: forward, 5′-ACGCTGTTTCGGACCCAG-3′; reverse, 5′-AGGGCGTATTCTAGCTGCTGTT-3′; and probe, 5′-TCATCCGGAGCTGCGAGGCC-3′. A reference curve to quantify XCR1 was generated by amplifying serial dilutions of cDNA derived from unstimulated $CD8^+$ lymphocytes to cover the range of 1–250 ng. Each assay included duplicate standard curve samples, a no template control, and triplicate cDNA samples. All samples with coefficient of variation >10% were retested. The XCR1 mRNA level in each sample was expressed as the amount of XCR1 mRNA normalized against the housekeeping gene *GAPDH* mRNA used as internal control gene.

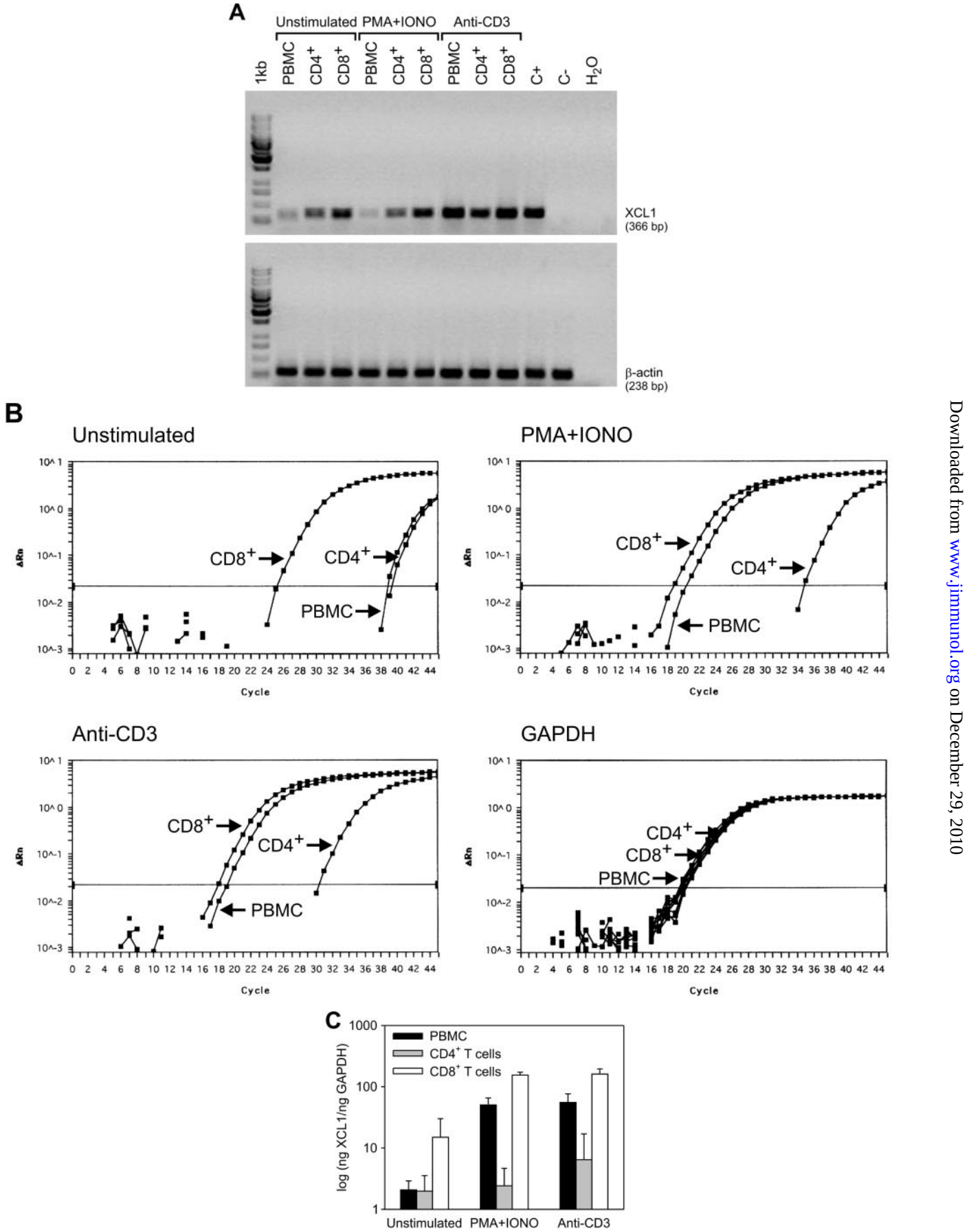

FIGURE 1. PCR and real-time PCR analysis of XCL1 expression in different lymphocyte subsets. *A*, Representative profile of XCL1 mRNA expression by nonquantitative PCR in PBMC, purified $CD4^+$ cells, and purified $CD8^+$ cells before (unstimulated) and after in vitro polyclonal activation (PMA/

Production of anti-XCL1 mAb

Given the paucity of available commercial reagents to set up a sandwich ELISA for human XCL1, we generated anti-XCL1 mAbs in our laboratory. Female BALB/c mice, 8–10 wk old, were immunized with human rXCL1 (Chemicon, St. Louis, MO; 10 μg i.p in CFA). Following boosting 15 days later, splenocytes from immunized mice were fused with myeloma cells in the presence of 50% polyethylene glycol 4000 and cloned. Over 100 primary hybridomas were obtained and were screened by ELISA and Western blotting using a human XCL1-GST fusion protein as a substrate (35). Thirty anti-XCL1 Ab-producing clones were stabilized; among them, seven clones were also tested for the ability to inhibit XCL1 chemotactic activity in an in vitro NK cell migration assay (in collaboration with P. Allavena, M. Negri Institute, Milan, Italy) and were able to neutralize XCL1 activity (data not shown). Five of these clones were grown as ascites in pristane-primed BALB/c mice; the ascitic fluid was precipitated in saturated ammonium sulfate and purified by dialysis against saline solution, and their Ab contents were evaluated with mouse Ig NL RID kit (Bioline, Birmingham, U.K.).

ELISA

The production of XCL1 in culture SN was evaluated by a homemade sandwich ELISA. A polyclonal rabbit anti-human XCL1 Ab (PeproTech, London, U.K.) was used as a capture Ab and coupled to the wells of polyethylene microtiter plates (Falcon, Grenoble, France; 5 μg/ml in carbonate/bicarbonate buffer, pH 9.6) as described previously (36). SN aliquots were then added to individual wells in triplicate; after overnight incubation at 4°C, the wells were extensively washed with PBS-BSA, and the anti-XCL1 mAb produced in our laboratory was added as a secondary Ab (10 ng/ml). After 4-h incubation at room temperature and extensive washings, an HRP-conjugated anti-mouse IgG (Amersham, Freiburg, Germany) was added as revealing Ab; HRP was visualized by incubation with *O*-phenylenediamine dihydrochloride tablets (Sigma Fast; Sigma-Aldrich), and OD was finally measured at 450 nm using a multiscan ELISA reader. Preliminary experiments showed that the detection limit of this ELISA was 10 pg/ml. To calculate the amount of XCL1 present in the SN, the absorbance values were plotted against a standard curve prepared using serial 2-fold dilutions of human rXCL1 in PBS-3% BSA.

Cytofluorometric analysis

Cytofluorometric analysis was performed as reported previously (37) on an XL cytofluorometer (Coulter Electronics, Hialeah, FL) using the Expo32 software. At least 15,000 cells were collected in each fluorescence histogram; the negative control settings were determined by using labeled Ig of the corresponding isotype. The percentages of the $CD3^+CD8^+CD5^-$ and $CD3^+CD8^+CD5^+$ subpopulations in PBMC were evaluated by triple fluorescence using the following mAb combination: anti-CD3-PerCP, anti-CD8-PE, and anti-CD5-FITC (all from Coulter-Immunotech). The phenotypic profile of the different subpopulations obtained at different steps of the fractionation procedures was analyzed using the following mAb: anti-CD3-FITC, anti-CD8-PE, anti-CD4-PE (all from BD Biosciences), anti-CD5-FITC and anti-CD62L-FITC (both from Coulter-Immunotech). The surface expression of CD8$\alpha\beta$ and CD8$\alpha\alpha$ on $CD3^+CD8^+CD5^-$ and $CD3^+CD8^+CD5^+$ subpopulations was evaluated by single immunofluorescence staining with an anti-CD8 mAb recognizing the α-chain of CD8 (thus staining all $CD8^+$ cells) and an anti-CD8 mAb recognizing a CD8 epitope generated by coupling of the α- and β-chains (which stains only CD8$\alpha\beta$-expressing lymphocytes); both mAb were purchased from Coulter-Immunotech. The percentage of cells expressing the $\alpha\alpha$ form of CD8 was then calculated as the difference between values obtained with the anti-CD8α mAb and values obtained with the mAb recognizing the $\alpha\beta$-associated epitope (38).

RNase protection assay

Chemokine expression in $CD3^+CD8^+CD5^-$ and $CD3^+CD8^+CD5^+$ cells was analyzed using the RiboQuant MultiProbe mRNase protection assay (BD PharMingen, San Diego, CA). The Multiprobe template set specific for the detection of human XCL1, CCL2, CCL3, CCL5, CXCL8, and CXCL10 mRNA was synthesized by BD PharMingen. Briefly, antisense RNA probes were generated from DNA templates using T7 DNA-dependent polymerase, in the presence of [α-^{32}P]UTP (Amersham Pharmacia Biotech; sp. act., 10 μCi/μl). Labeled probes were hybridized with total RNA (10 μg) overnight at 56°C; nonhybridized RNA was digested with RNase according to the manufacturer's instructions. RNase-protected probes were resolved by 5% SDS-PAGE, and the gel was air-dried and finally exposed to XAR film (Eastman Kodak, Rochester, NY) at −70°C. The identity of each protected fragment was established by analyzing its migration distance against a standard curve of the migration distance vs the log nucleotide length for each undigested probe. To quantify chemokine mRNA expression, the gel was analyzed by Instant Imager (Camberra-Packard, Grove Hills, IL), and the chemokine/GAPDH ratio was calculated.

Statistical analysis

Data were managed by StatGraphics software (Statgraphics Statistical Graphics System, version 2.6, Rockville, MD). The correlation coefficient was calculated by simple regression analysis, and Wilcoxon's test was used to compare quantitative variables. Unless otherwise specified, results were expressed as the mean ± 1 SD.

Results

XCL1 expression in different T cell subsets

By a conventional PCR assay, a message for XCL1 was detected in both unstimulated and mitogen-activated PBMC as well as in purified $CD4^+$ and $CD8^+$ populations (Fig. 1*A*). The message was barely evident in freshly isolated PBMC and was strongly enhanced by in vitro culture with anti-CD3 mAb for 30 h; surprisingly, PMA/ionomycin stimulation was not apparently associated with a significant change in XCL1 band intensity (Fig. 1*A*).

By real-time PCR (Fig. 1, *B* and *C*), a low constitutive expression of the XCL1 gene was observed in freshly isolated PBMC; anti-CD3 and PMA/ionomycin activation were both associated with a strong increase in the specific message (Fig. 1*C*, ■). When $CD4^+$ and $CD8^+$ lymphocytes were isolated by positive selection, only a scanty XCL1 message could be observed in $CD4^+$ T cells, which did not substantially increase following OKT3 or PMA/ionomycin stimulation (Fig. 1*C*, ▨). In contrast, high levels of XCL1 mRNA were detectable in freshly isolated $CD8^+$ T cells, as clearly shown by the fact that the amplification curves of $CD8^+$ lymphocytes intersected the threshold line at a much lower number of PCR cycles, compared with PBMC and $CD4^+$ cells (Fig. 1*B*); as shown in Fig. 1*C* (□), real-time PCR figures were significantly higher than in unfractionated PBMC or purified $CD4^+$ lymphocytes. Moreover, in vitro activation of purified $CD8^+$ cells with either PMA/ionomycin or anti-CD3 mAb was associated with a >1 log increase in XCL1 expression, compared with unstimulated cells (Fig. 1*C*).

XCL1 expression has been reported in activated $\gamma\delta^+$ T lymphocytes (17, 18). In fact, when XCL1 expression was compared by real-time PCR in purified TCR $\alpha\beta$- and $\gamma\delta$-expressing T cells, XCL1 expression was observed in both populations (Fig. 2). On a quantitative basis, however, the XCL1 message was higher in $\gamma\delta^+$

ionomycin and anti-CD3). C+, XCL1-expressing positive control; C−, the MCF7 cell line, not expressing XCL1; markers are shown in the *first left lane*. The β-actin control for RNA quality is shown at the *bottom*. *B*, The panel shows the real-time PCR amplification plots obtained in a single representative experiment for XCL1 expression analysis of PBMC, $CD4^+$ T cells, and $CD8^+$ T cells in basal conditions (unstimulated) and after PMA/ionomycin or anti-CD3 mAb stimulation; the amplification plots of the same samples for the housekeeping gene GAPDH are also reported. The number of PCR cycles was plotted vs the change in normalized reporter signal (ΔRn), as detailed in *Materials and Methods*. *C*, Analysis of XCL1 expression by real-time PCR in unstimulated and polyclonally activated PBMC (■), purified $CD4^+$ cells (▨), and purified $CD8^+$ cells (□). Results are expressed as the ratio between the expression of the XCL1 gene and the expression of the GAPDH gene, and represent the mean ± SD of 10 (PBMC) and seven experiments ($CD4^+$ and $CD8^+$ cells).

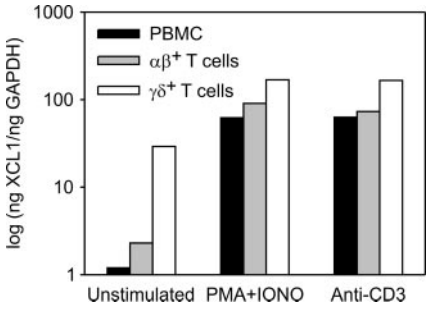

FIGURE 2. Real-time PCR analysis of XCL1 expression in unstimulated and polyclonally activated TCR $\alpha\beta$- and $\gamma\delta$-expressing T lymphocytes. Results were expressed as the ratio between the expression of the XCL1 gene and the expression of the GAPDH gene; one representative experiment is shown.

than $\alpha\beta^+$ T cells; indeed, constitutive expression was mostly observed in $\gamma\delta^+$ T lymphocytes, whereas it was much lower in the $\alpha\beta^+$ population (Fig. 2).

XCL1 synthesis by different T cell subsets

Quantitative RNA expression data were also confirmed at the protein level by measuring XCL1 production in culture SN of different cell populations by a sensitive ELISA set up in our laboratory. As shown in Fig. 3*A*, XCL1 production by unstimulated PBMC was low and was greatly increased following in vitro activation; on the other hand, constitutive XCL1 synthesis by purified $CD4^+$ T cells was also low, and it was not substantially changed by anti-CD3 or

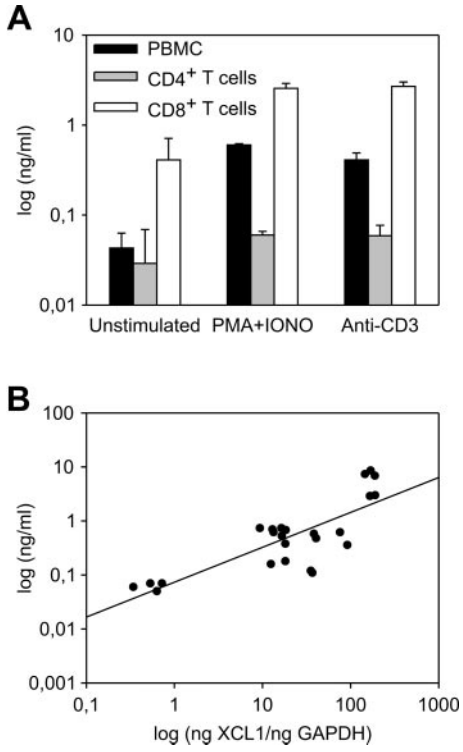

FIGURE 3. XCL1 production by different lymphocyte subsets. *A*, XCL1 contents in culture SN of unstimulated and polyclonally activated PBMC (■), purified $CD4^+$ cells (▨), and purified $CD8^+$ cells (□) was measured by ELISA. Unstimulated cells were cultured for 30 h in the absence of mitogens. *B*, Correlation between XCL1 expression as evaluated by real-time PCR and XCL1 synthesis in culture SN. The diagram pooled results obtained in both unstimulated and polyclonally activated PBMC, $CD4^+$, and $CD8^+$ cells.

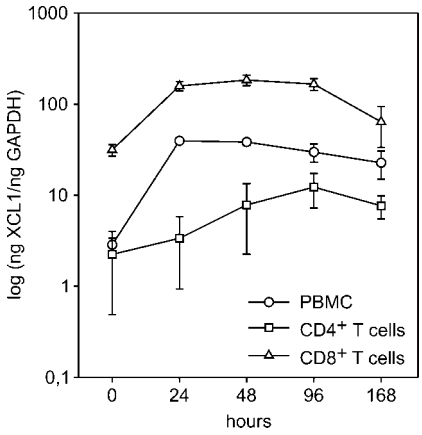

FIGURE 4. Kinetics of XCL1 expression in different lymphocyte populations, as evaluated by real-time PCR. Results were expressed as detailed in Fig. 1*C* and represent the mean ± SD of three consecutive experiments.

PMA/ionomycin stimulation (Fig. 3*A*). On the contrary, in both the absence and the presence of polyclonal activators, $CD8^+$ T cells produced ~50-fold the amount of XCL1 released by $CD4^+$ T lymphocytes in the corresponding conditions (Fig. 3*A*). As shown in Fig. 3*B*, the real-time PCR data showed a good linear correlation with in vitro XCL1 production ($r = 0.827$; $p < 0.05$).

Kinetics of XCL1 expression in different T cell subsets

We then addressed the kinetics of XCL1 expression. As shown in Fig. 4, anti-CD3 stimulation of PBMC was associated with a rapid increase in XCL1 expression from baseline values, and levels remained substantially stable over 3 days of culture in the presence of rIL-2, slowly declining thereafter (Fig. 4). A modest increase in XCL1 expression was also observed when purified $CD4^+$ T cells were activated and cultured in the presence of rIL-2 (Fig. 4), but the values reached in unfractionated PBMC or purified $CD8^+$ lymphocytes were not attained. Similar results were obtained when long term $CD4^+$ cell lines were tested over a 7-wk period, and when >20 different $CD4^+$ T cell clones were analyzed for XCL1 expression (data not shown). On the other hand, $CD8^+$ cells showed a sharp increase in XCL1 expression as early as 24 h following anti-CD3 activation, which reached a plateau at 2–4 days, slowly declining thereafter (Fig. 4). In these experiments we could also confirm data by Olive et al. (39) on the differential effect of anti-CD28 costimulation on XCL1 expression by different T cell subsets; in fact, the addition to anti-CD3-stimulated $CD4^+$ cell cultures of an anti-CD28 mAb was associated with down-modulation of the modest levels of XCL1 expression, whereas XCL1 expression by $CD8^+$ lymphocytes was substantially refractory to the presence in culture of the anti-CD28 mAb (data not shown).

XCL1 expression in different $CD8^+$ T cell subsets

These data clearly indicated that $CD3^+CD8^+$ T cells were the major XCL1-producing population within TCR $\alpha\beta$-expressing T cells and produced this chemokine both constitutively and following polyclonal activation. It is known that within $CD3^+CD8^+$ T cells a minor subset can be distinguished, which is characterized by the lack of surface CD5 expression (40–42). We thus separated $CD3^+CD8^+$ cells on the basis of CD5 expression; as shown in Fig. 5, the XCL1 expression recorded in $CD3^+CD8^+$ lymphocytes was mostly contributed to by the $CD5^-$ subset, as constitutive and activation-induced XCL1 expression were ~5 and 12 times higher, respectively, in $CD3^+CD8^+CD5^-$ cells than in the CD5-expressing counterpart. These figures were also confirmed at the protein

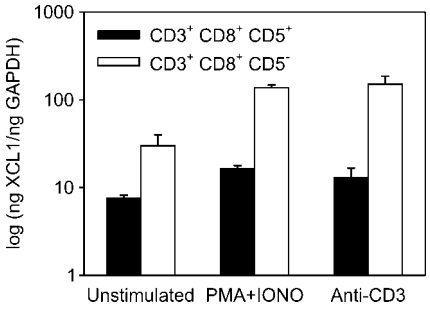

FIGURE 5. Real-time PCR analysis of XCL1 expression in $CD3^+CD8^+$ T cells expressing and not expressing the CD5 marker. Purified $CD3^+CD8^+CD5^+$ (■) and $CD3^+CD8^+CD5^-$ (□) lymphocytes were analyzed immediately after isolation and following in vitro polyclonal activation. Results were expressed as indicated in Fig. 1*C* and represent the mean ± SD of five consecutive experiments.

level; in fact, when we measured XCL1 contents in culture SN by ELISA, in both unstimulated and activated cells XCL1 production was significantly higher in $CD3^+CD8^+CD5^-$ cells than in $CD3^+CD8^+CD5^+$ lymphocytes (Table I). The separation protocol for $CD3^+CD8^+CD5^-$ cell isolation, which entailed a positive selection step with the anti-CD3 mAb, did not account for this difference; in fact, when the $CD3^+CD8^+CD5^+$ cells were also subjected, before testing, to positive selection with anti-CD3, no change in constitutive XCL1 expression was observed compared with $CD3^+CD8^+CD5^+$ lymphocytes that did not undergo this procedure (data not shown). The constitutive expression of XCL1 in $CD3^+CD8^+CD5^-$ cells T cells was equal to or even higher than that with $\gamma\delta^+$ T cells (see Figs. 2 and 5). Thus, XCL1 expression by $\alpha\beta^+$ T cells seemed to be relatively restricted to this small subset, which accounts for ~3–10% of the $CD8^+$ T cells in the circulation of healthy donors (40, 42). Although this population has been characterized to some extent, information on its phenotypic and functional properties is incomplete, and its function and physiologic significance are unknown.

Phenotypic characterization of $CD3^+CD8^+CD5^-$ lymphocytes

In view of this, we addressed some unexplored phenotypic properties of $CD8^+CD5^-$ T cells. The size of this subset in the different lymphoid compartments was small; in peripheral blood, according to previously published data (41, 42), the percentage of $CD3^+CD8^+CD5^-$ cells within the CD8-expressing population was 5.2 ± 2.8 (range, 10.2–1.0); the size of this subset was significantly lower in lymph nodes (1.3 ± 0.8; range, 2.5–0.5; $p < 0.01$, according to the Mann-Whitney test) and tonsils (3.5 ± 3.0; range, 7.9–1.0); in these latter, probably due to the small number of samples examined, the difference from PBMC was not significant ($p = 0.43$).

It is known that the CD8 Ag may be expressed on the cell surface in two molecular forms, as a homodimer composed of two α-chains or as a heterodimer composed of an α- and a β-chain (43, 44); the CD8$\alpha\beta$-expressing population is much more represented in the circulation (38, 43, 44). To evaluate the expression of these two CD8 forms at the surface of $CD3^+CD8^+CD5^-$ lymphocytes and in view of the absence of an anti-CD8 mAb specifically directed against the CD8β chain, we were forced to calculate the proportion of CD8$\alpha\alpha$-expressing cells as the difference between the figures obtained with two mAb recognizing different epitopes of the CD8 molecule. As shown in Fig. 6*A*, virtually all $CD3^+CD8^+CD5^+$ and $CD3^+CD8^+CD5^-$ lymphocytes stained with an anti-CD8α mAb, whereas an anti-CD8 mAb recognizing a CD8 epitope generated by coupling of the α- and β-chains recognized all $CD3^+CD8^+CD5^+$ cells, but only a fraction of $CD3^+CD8^+CD5^-$ lymphocytes. As a consequence, we could conclude that a significantly higher ($p < 0.01$) proportion of $CD3^+CD8^+CD5^-$ cells expressed the $\alpha\alpha$ form of the CD8 molecule compared with the $CD5^+$ counterpart, which, as expected (38, 43, 44), mostly expressed the $\alpha\beta$ variant of this coreceptor (Fig. 6*B*).

Table I. *XCL1 production by unstimulated and stimulated $CD3^+CD8^+CD5^+$ and $CD3^+CD8^+CD5^-$ lymphocytes*[a]

	$CD3^+CD8^+CD5^+$	$CD3^+CD8^+CD5^-$
Unstimulated	0.24 ± 0.11[b]	1.60 ± 0.60[c]
PMA	0.63 ± 0.14	6.34 ± 0.31[c]
Anti-CD3	0.67 ± 0.25	6.26 ± 0.35[c]

[a] $CD3^+CD8^+$ lymphocytes were separated according to CD5 expression as outlined in *Materials and Methods*; the resulting $CD3^+CD8^+CD5^+$ and $CD3^+CD8^+CD5^-$ populations were cultured in vitro alone and in the presence of PMA (4 h) or anti-CD3 mAb (30 h). At the end of the incubation period, SN were recovered and tested for XCL1 contents by ELISA.

[b] Results were expressed as nanograms per milliliter (mean ± SD of four consecutive experiments).

[c] $p < 0.01$ compared to $CD3^+CD8^+CD5^+$ cells.

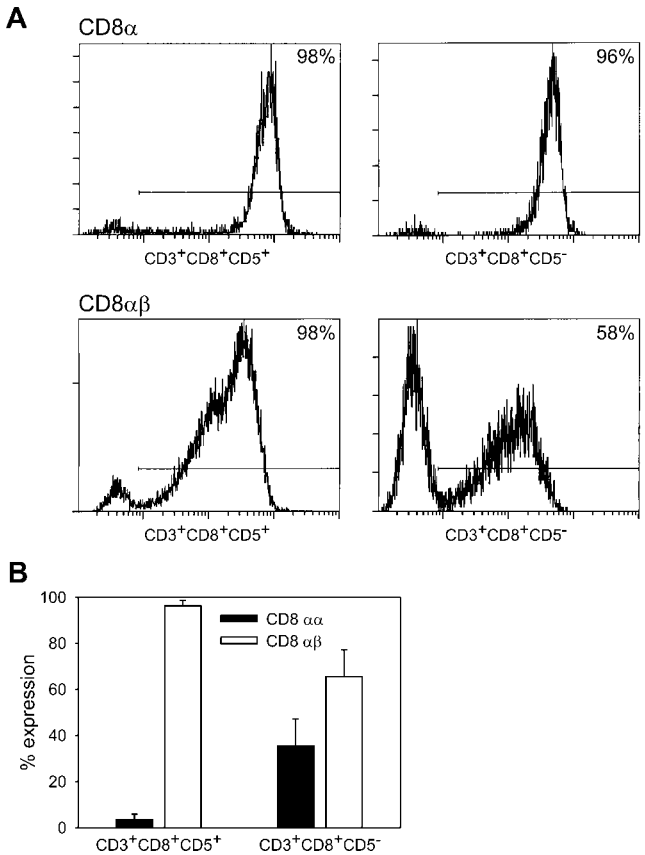

FIGURE 6. Cytofluorometric analysis of CD8 expression in $CD3^+CD8^+CD5^+$ and $CD3^+CD8^+CD5^-$ lymphocyte subsets. The $CD3^+CD8^+CD5^+$ and $CD3^+CD8^+CD5^-$ populations were purified and stained with an anti-CD8 mAb recognizing the α-chain of CD8 (which stains all $CD8^+$ cells) or an anti-CD8 mAb recognizing a CD8 epitope generated by coupling of the α- and β-chains (which only stains CD8$\alpha\beta$-expressing lymphocytes). The percentage of cells expressing the $\alpha\alpha$ form of CD8 was then calculated as the difference between the two values obtained. *A*, Results obtained in a representative experiment; the percent expression for each mAb is indicated inside each fluorogram. *B*, Summary of the results obtained in seven consecutive experiments (mean ± SD).

In previous investigations (40) we showed that $CD3^+CD8^+CD5^-$ lymphocytes did not display a univocal memory/naive phenotype, as ~30% of them expressed CD45RO, and ~60% expressed CD45RA, which are considered putative markers of memory and virgin cells, respectively. To further clarify this aspect, we addressed L-selectin expression on $CD3^+CD8^+CD5^-$ and $CD3^+CD8^+CD5^+$ cell surfaces. As shown in Fig. 7, CD62L, which is usually associated with a nonactivated/naive phenotype and is considered a major receptor for lymphocyte homing to lymph nodes, was expressed at a significantly lesser extent in $CD3^+CD8^+CD5^-$ lymphocytes than in the $CD5^+$ population (Fig. 7*B*; $p < 0.01$).

Finally, we compared the expression of the XCL1 receptor, XCR1, by $CD3^+CD8^+CD5^-$ and $CD3^+CD8^+CD5^+$ cells by both conventional and real-time PCR analysis. As shown in Fig. 8, by the former technique XCR1 expression was barely detectable in unstimulated PBMC, whereas a more distinct band was present in purified $CD8^+$ lymphocytes as well as in $CD3^+CD8^+CD5^-$ and $CD3^+CD8^+CD5^+$ subpopulations. Upon anti-CD3 activation, XCR1 expression was clearly evidenced in all the above populations, but not in two control cell lines, a Kaposi sarcoma cell line (KS-IMM) and the mammary adenocarcinoma cell line MCF7 (Fig. 8). Real-time PCR analysis showed a significant difference in XCR1 expression between $CD3^+CD8^+CD5^+$ cells (6.17 ± 0.084 ng of XCL1/ng GAPDH) and $CD3^+CD8^+CD5^-$ cells (6.95 ± 0.082; $p < 0.01$). Thus, XCR1 expression also seems to discriminate between these two $CD8^+$ lymphocyte subsets.

Analysis of CD5 expression in $CD3^+CD8^+CD5^-$ lymphocytes

CD5 expression on T lymphocytes occurs during thymocyte orthogenesis (45), and several studies demonstrated that its expression may be involved in positive and negative selection processes (46, 47). Nevertheless, no information exists on the status of the CD5 gene in $CD8^+CD5^-$ T cells; in other words, is it irreversibly shut off or may it be reactivated under certain experimental conditions? To address this issue, we isolated $CD3^+CD8^+CD5^-$ T cells and tested the presence of CD5 mRNA before and after in vitro activation. As shown in Fig. 9, PCR analysis did not show any CD5 message in either freshly isolated or anti-CD3 mAb- or PMA/ionomycin-stimulated $CD3^+CD8^+CD5^-$ cells, whereas a clear message was evident by both PCR (Fig. 9) and Northern blotting (not shown) in other CD5-expressing populations; furthermore, no CD5 Ag expression could be recorded on the surface of mitogen-activated $CD3^+CD8^+CD5^-$ cells by cytofluorographic analysis (data not shown).

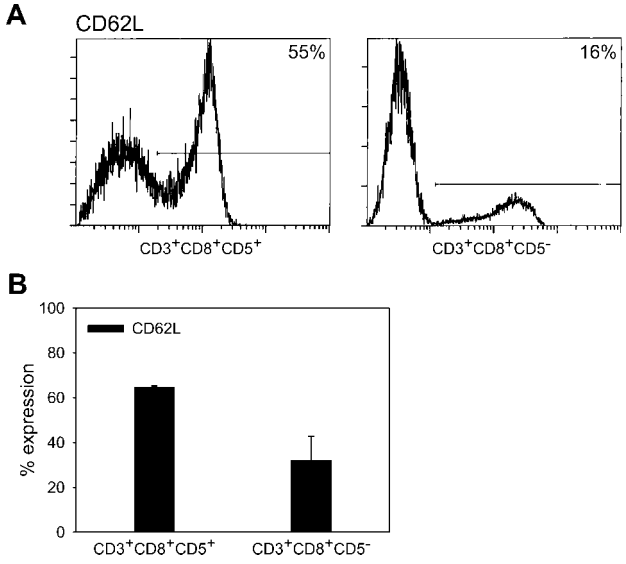

FIGURE 7. Cytofluorometric analysis of CD62L expression in $CD3^+CD8^+CD5^+$ and $CD3^+CD8^+CD5^-$ lymphocyte subsets. Results obtained in a single representative experiment are shown in the fluorograms (*A*); the mean ± SD of five consecutive experiments are summarized in *B*.

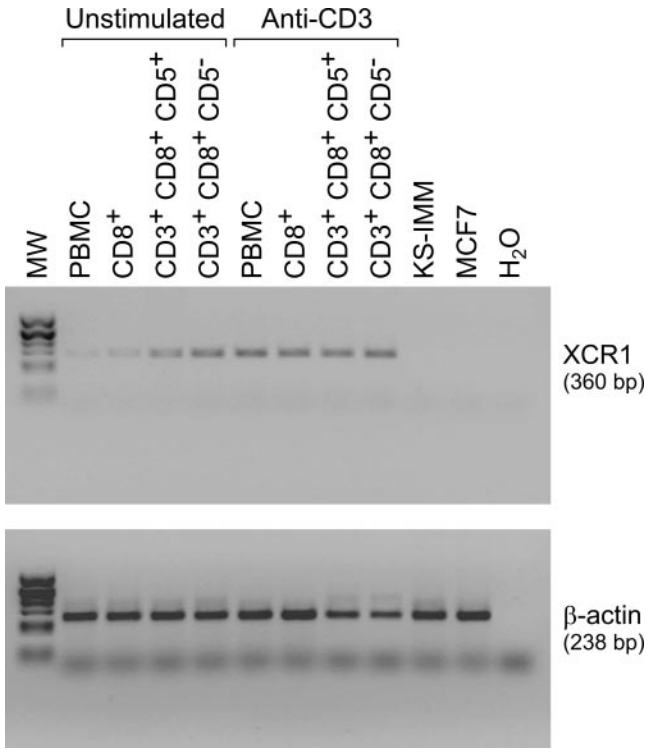

FIGURE 8. PCR analysis of XCR1 expression in unfractionated PBMC, purified $CD8^+$ cells, and $CD3^+CD8^+CD5^+$ and $CD3^+CD8^+CD5^-$ subsets. The relevant cell populations were purified as described in *Materials and Methods*, and RNA was extracted either immediately or following in vitro polyclonal activation with anti-CD3 mAb for 30 h. KS-IMM and MCF7 depict results obtained, respectively, with a Kaposi sarcoma cell line (provided by Dr. A. Albini, Genua, Italy) and the human mammary adenocarcinoma MCF7 cell line. Molecular markers (MW) are shown in the *first left lane.*

α- and β-chemokine expression in $CD3^+CD8^+CD5^-$ T cells

We finally compared the abilities of $CD3^+CD8^+CD5^+$ and $CD3^+CD8^+CD5^-$ cells to express a panel of α and β chemokines by RNase protection assay; as a control, we also included evaluation of XCL1 expression by this same approach. As shown in Fig. 10, no difference in constitutive or activation-induced expression of the α-chemokines CXCL8 and CXCL10 was observed between

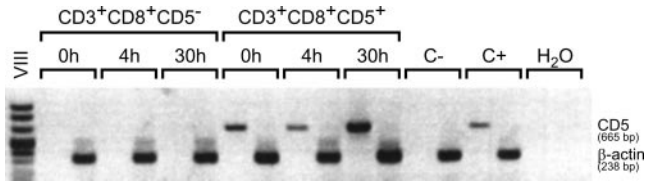

FIGURE 9. PCR analysis of CD5 expression in $CD3^+CD8^+CD5^+$ and $CD3^+CD8^+CD5^-$ lymphocytes. The relevant subsets were purified as described in *Materials and Methods*, and RNA was extracted either immediately or following in vitro polyclonal activation with PMA/ionomycin for 4 h or anti-CD3 mAb for 30 h. C−, Results obtained with the MCF7 cell line, not expressing CD5; C+, unfractionated PBMC as a positive control. Molecular markers are shown in the *first left lane*.

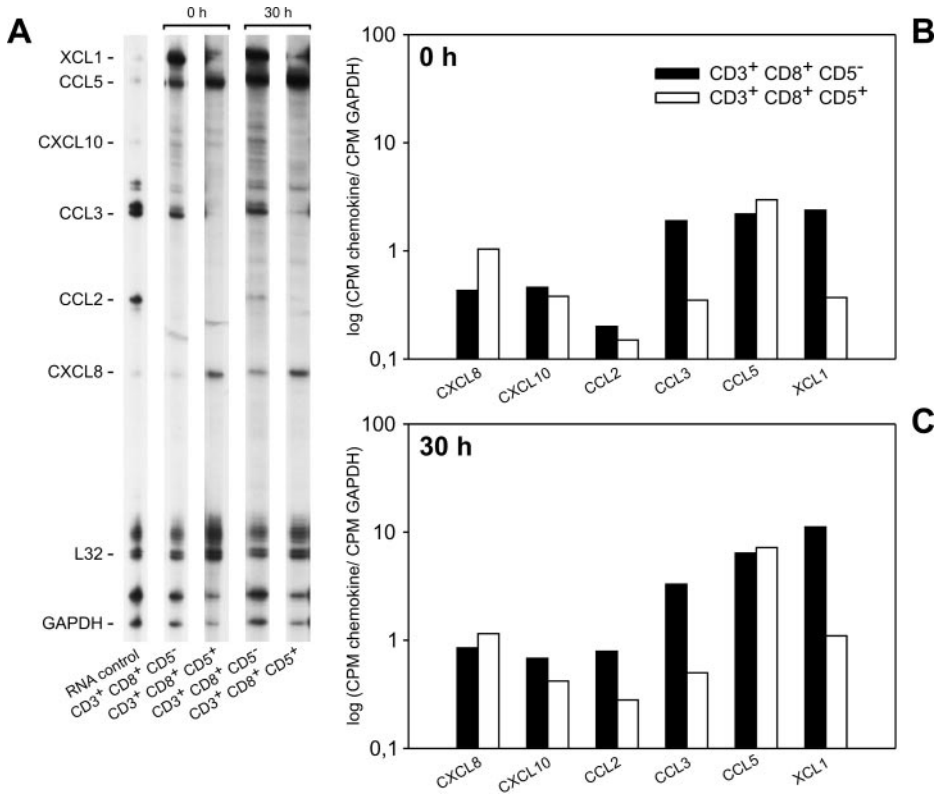

FIGURE 10. RNase protection assay for analysis of chemokine expression in $CD3^+CD8^+CD5^+$ and $CD3^+CD8^+CD5^-$ lymphocytes. *A*, Results obtained in a representative experiment are shown. RNA was extracted immediately after cell isolation (0 h) and following in vitro activation (30 h). Chemokine controls are shown in the *first left lane*. Densitometric analysis of the ratio between the expression of the individual chemokines and the GAPDH gene is shown in *B* for unstimulated cells and in *C* for cells activated in vitro with anti-CD3 mAb.

$CD3^+CD8^+CD5^+$ and $CD3^+CD8^+CD5^-$ cells; in addition, the constitutive and activation-induced expression of the β- chemokines CCL2 and CCL5 was roughly comparable in the two subsets. In contrast, constitutive CCL3/macrophage inflammatory protein-1α expression was much higher in freshly isolated $CD3^+CD8^+CD5^-$ lymphocytes than in the $CD5^+$ counterpart (Fig. 10*B*); this difference between the two subsets was also evident following in vitro anti-CD3 mAb stimulation of the cells (Fig. 10*C*). The preferential expression of CCL3 in $CD3^+CD8^+CD5^-$ cells paralleled the behavior observed for XCL1 (Fig. 10, *B* and *C*), which was confirmed by RNase protection assay data obtained by real-time PCR and ELISA.

Discussion

In the world of chemokines, the γ chemokine lymphotactin/XCL1 has been long regarded as a minor component, not only in view of its poor cysteine endowment compared with chemokines belonging to CC and CXC families, but also because of its limited activities on NK and $CD8^+$ T cells. Nevertheless, the interest in XCL1 has recently received a new impetus due to the identification of its receptor (48) and to several investigations that indicated its possible role as a potent adjuvant in cancer immunotherapy (25–29, 49–51). Data are also rapidly accumulating in other immunopathologic settings, and XCL1 has been shown to be involved in some autoimmune disorders and in transplant rejection in both experimental models and humans (52–56). Two major problems still need to be solved. Firstly, although the expression of XCL1 has been described virtually in all lymphocyte populations, including $CD8^+$ lymphocytes (7–12), $CD4^+$ lymphocytes (19–21), NK cells (7, 13, 14), and $\gamma\delta^+$ T cells (17, 18) under a variety of experimental conditions, the available data are mostly based on nonquantitative PCR analyses, and no thorough comparison of the actual XCL1 synthesis and/or the expression in different T cell populations was attempted. Secondly, although clear XCL1 effects other than lymphocyte migration were described on several cell types, including $CD4^+$ T cells (22, 57), this issue is as yet incompletely addressed, and the position of XCL1 within the cytokine/chemokine network is still elusive.

This article intended to give an answer to the first issue by evaluating in a quantitative manner the production of XCL1 by different T cell populations. By a nonquantitative PCR assay, our data confirmed previous experiments (7–19) and showed that the constitutive and activation-induced XCL1 message detected in PBMC was also present in both $CD4^+$ and $CD8^+$ lymphocytes. However, comparison of data obtained by conventional PCR (Fig. 1*A*) and real-time PCR (Fig. 1*C*) clearly demonstrated how misleading the former may be; in fact, even though XCL1 expression was greatly potentiated by in vitro PBMC stimulation with anti-CD3 mAb, no apparent effect of PMA/ionomycin on PBMC could be recorded by a conventional PCR assay (Fig. 1*A*), which was instead evidenced by quantitative molecular analysis (Fig. 1*C*) and confirmed by ELISA (Fig. 3). In addition, when XCL1 expression was addressed at the molecular level by real-time PCR and by a sensitive ELISA at the protein level, constitutive XCL1 expression was almost 2 log higher in $CD8^+$ T cells compared with $CD4^+$ lymphocytes; a similar gap between the two lymphocyte subsets was maintained following in vitro polyclonal T cell activation. XCL1 production was not greatly enhanced by in vitro $CD4^+$ cell culture, nor was substantial XCL1 synthesis observed in established $CD4^+$ cell clones; nonetheless, our quantitative analysis (data not shown) confirmed observations made by Olive et al. (39) and, more recently, by Cristillo et al. (58) showing that CD28 engagement could only modulate the scanty XCL1 expression of $CD4^+$ cells without substantially affecting the synthesis by $CD8^+$ lymphocytes. On the whole, our and previous findings (39, 58) are in contrast with the observations by Hautamaa et al. (59), who found a down-regulating effect of CD28 costimulation on XCL1 expression in both murine $CD4^+$ and $CD8^+$ lymphocytes; whether

this apparent discrepancy is due to interspecies variability or differences in culture conditions and detection techniques will be clarified by future work.

The major contribution to XCL1 production within the $CD8^+$ subpopulation was given by a $CD8^+$ subset that lacks expression of the CD5 surface marker. In this small $CD3^+CD8^+CD5^-$ subpopulation, constitutive XCL1 expression was equal to or even greater than that observed in $\gamma\delta^+$ T lymphocytes, another T cell subset known to steadily produce XCL1 (17, 18). The high constitutive and activation-induced synthesis of XCL1 shown by the $CD3^+CD8^+CD5^-$ cell population was not due to residual $\gamma\delta^+$ cell contamination, as purification procedures entailed a positive selection step of $CD8^+$ cells, and $\gamma\delta^+$ T lymphocytes mostly do not express this marker. Moreover, cytofluorographic analysis of $CD3^+CD8^+CD5^-$ cells showed a $\gamma\delta^+$ T cell contamination never exceeding 1%. Nor could our data be attributed to the residual presence within the $CD3^+CD8^+CD5^-$ population of NK cells, which do express CD8, in view of the expression of the CD3 marker in >99% of the cells obtained at the end of the purification procedure. Thus, we could reasonably conclude that within TCR $\alpha\beta^+$ T lymphocytes XCL1 is mostly produced by $CD8^+$ T cells that lack surface CD5 expression, and that the contribution to its synthesis by different TCR $\alpha\beta$-expressing T cell subsets, namely $CD4^+$ lymphocytes, is negligible.

These results prompted us to investigate the properties of the major XCL1-producing T cell population, which are largely unexplored; even though the size of this population is small, its dimensions, in fact, equal those of $\gamma\delta^+$ T lymphocytes or NK cells. Previous work showed that $CD3^+CD8^+$ T lymphocytes that lack surface CD5 expression are increased in the circulation of bone marrow transplant recipients (60, 61) and HIV-infected patients with advanced disease progression (40). A limited characterization of this subset (40) revealed that the $CD3^+CD8^+CD5^-$ cells had a mixed naive/memory phenotype, an impaired in vitro response to mitogens and Ags, and poor ability to generate alloreactive CTL; on the other hand, the $CD3^+CD8^+CD5^-$ population, although devoid of NK activity, was endowed with mitogen-induced cytotoxic potential (40). The present data confirm and extend these observations and show that $CD3^+CD8^+CD5^-$ lymphocytes express molecules commonly associated with a noncommitted/naive phenotype such as CD62L to a lesser extent than the $CD5^+$ counterpart. In addition, the $CD3^+CD8^+CD5^-$ cells show preferential expression of the $\alpha\alpha$ form of the CD8 molecule compared with the canonical $CD8^+$ population. This finding is somewhat surprising and may help in explaining some experimental and/or clinical observations. The $\alpha\alpha$ form of CD8 is mostly expressed on NK cells (43, 62) and is usually associated with a poor proliferative response to mitogenic stimulation and preferential display of non-MHC-restricted cytotoxic activity (43, 63). Indeed, in several repeated attempts we never succeeded in stabilizing in vitro long term $CD3^+CD8^+CD5^-$ lines or clones; the inability of these cells to undergo substantial in vitro expansion was apparently not due to the production of immunomodulatory cytokines, such as TGF-β (data not shown). If transferred to a clinical setting, these observations may at least partly account for the observed impairment of the $CD8^+$ cell function in AIDS patients (64); besides the inefficient cooperation by $CD4^+$ lymphocytes, in fact, in these patients the increment in a compartment of functionally inert $CD3^+CD8^+CD5^-$ cells (40) could also contribute by this pathway to the overall dysfunction of cytotoxic responses. Moreover, in view of the special ability of these cells to constitutively produce XCL1, and given the ability of this latter to down-regulate Th1 cell function (22), the expansion of $CD3^+CD8^+CD5^-$ cells in the circulation of AIDS patients could be a further element contributing to the general immune impairment associated with HIV infection.

The significance of the $CD3^+CD8^+CD5^-$ subset within the physiology of the immune response remains unclear. As far as we could document, the $CD3^+CD8^+CD5^-$ phenotype is highly stable, as no CD5 messenger expression follows in vitro cell activation. This observation is in contrast with data obtained in mice by Muller et al. (65), who found the expression of CD5 Ag in in vitro activated intraepithelial $\alpha\beta^+$ $CD8^+$ T cells lacking CD5 expression; whether this divergent behavior is due to differences between humans and mice or to special features of mucosa-associated $CD3^+CD8^+CD5^-$ lymphocytes is unclear. It was shown that CD5 expression at the cell surface may play a role during the complex itinerary of T cell maturation in the thymus (45–47); thus, the ontogenetic pathways followed by $CD3^+CD8^+CD5^-$ lymphocytes are also uncertain, and work will be needed to ascertain whether a subset with similar properties could also be identified in the thymic tissue. In this regard, the observed association of an increase in $CD3^+CD8^+CD5^-$ lymphocytes during immune system reconstitution in patients undergoing bone marrow transplantation (60, 61) also deserves attention.

Notwithstanding, this small subset of $CD8^+$ lymphocytes differs from the "orthodox" $CD8^+$ T cells not only in the lack of CD5 expression, but also in other phenotypic characteristics, such as the composition of the CD8 coreceptor and the expression of homing molecules such as L-selectin. In addition, $CD3^+CD8^+CD5^-$ cells express higher levels of the XCR1 receptor; thus, even though we did not address their chemotactic properties in response to XCL1, it is conceivable that their functional response could be more pronounced compared with the CD5-expressing counterpart. Some of these properties, such as the preferential expression of the $\alpha\alpha$ form of CD8 observed here and the ability of these cells to exert lectin-mediated cytotoxicity (40), would seem to suggest a transitional phenotype of the $CD3^+CD8^+CD5^-$ subset, sharing properties of T lymphocytes and NK cells. On the other hand, the $CD3^+CD8^+CD5^-$ population shows a particular profile of chemokine expression, in that not only it is a major source of XCL1, but it is also able to produce higher quantities of CCL3/macrophage inflammatory protein-1α, both constitutively and following in vitro activation, compared with the CD5-expressing $CD8^+$ counterpart. The significance of this observation is presently unclear, but it is interesting to recall that in murine models both XCL1 and CCL3 act synergistically with IFN-γ as a functional unit within the innate phase of immunity (23). These observations must be substantiated by more careful screening of the expression of a large panel of chemokines/cytokines by $CD3^+CD8^+CD5^-$ lymphocytes; in any case, further investigation will also be needed in different immunopathologic settings to clarify the role of this subset within the physiology of immune function. On the one hand, in fact, several observations would seem to point to its possible implication in antiviral immunity in view of its expansion in several viral infections (40, 66–68); on the other, the independent observations of an increase in this subset in renal transplant recipients undergoing kidney rejection (69) and of the possible role played by XCL1 in transplant rejection (54, 55) may indicate a new potential target in selected immunopathologic settings.

Acknowledgments

We are grateful to Drs. G. De Silvestro and P. Marson (from the Blood Transfusion Unit) kindly supplying the blood samples, and Dr. F. Comacchio (from the ENT Department) for providing tonsil samples. We also thank P. Gallo for artwork.

References

1. Baggiolini, M. 1998. Chemokines and leukocyte traffic. *Nature 392:565*.
2. Baggiolini, M. 2001. Chemokines in pathology and medicine. *J. Intern. Med. 250:91*.
3. Mantovani, A. 1999. Chemokines. Introduction and overview. *Chem. Immunol. 72:1*.
4. Zlotnik, A. and O. Yoshie. 2000. Chemokines: A new classification system and their role in immunity. *Immunity 12:121*.
5. Baggiolini, M., B. Dewald, and B. Moser. 1994. Interleukin-8 and related chemotactic cytokines-CXC and CC chemokines. *Adv. Immunol. 55:97*.
6. Rollins, B. J. 1997. Chemokines. *Blood 90:909*.
7. Hedrick, A. J., V. Sailor, D. Figueroa, L. Mizoue, Y. Xu, S. Menon, J. Abrams, T. Handel, and A. Zlotnik. 1997. Lymphotactin is produced by NK cells and attracts both NK cells and T cells in vivo. *J. Immunol. 158:1533*.
8. Hedrick, A. J., and A. Zlotnik. 1998. Molecule of the month: lymphotactin. *Clin. Immunol. Immunopathol. 87:218*.
9. Bianchi, G., S. Sozzani, A. Zlotnick, A. Mantovani, and P. Allavena. 1996. Migratory response of human natural killer cells to lymphotactin. *Eur. J. Immunol. 26:3238*.
10. Huang, H., F. Li, C. M. Cairns, J. R. Gordon, and J. Xiang. 2001. Neutrophilis and B cells express XCR1 receptor and chemotactically respond to lymphotactin. *Biochem. Biophys. Res. Commun. 281:378*.
11. Kelner, G. S., J. Kennedy, K. B. Bacon, S. Kleyensteuber, D. A. Largaespada, N. A. Jenkins, N. G. Copeland, J. F. Bazan, K. W. Moore, T. J. Schall, et al. 1994. Lymphotactin: a cytokine that represent a new class of chemokine. *Science 266:1395*.
12. Muller, S., B. Dorner, U. Korthauer, H. W. Mages, M. D'Apuzzo, G. Senger, and R. A. Kroczer. 1995. Cloning of ATAC, an activation-induced, chemokine-related molecule exclusively expressed in $CD8^+$ T lymphocytes. *Eur. J. Immunol. 25:1744*.
13. Inngjerdingen, M., B. Damaj, and A. A. Maghazachi. 2001. Expression and regulation of chemokine receptors in human natural killer cells. *Blood 97:367*.
14. Kennedy, J., A. P. Vicari, V. Saylor, S. M. Zurawski, N. G. Copeland, D. J. Gilbert, N. A. Jenkins, and A. Zlotnik. 2000. A molecular analysis of NKT cells: identification of a class-I restricted T cell-associated molecule (CRTAM). *J. Leukocyte Biol. 67:725*.
15. Vissers, J. L. M., F. C. Hartgers, E. Lindhout, M. B. M. Teunissen, C. G. Figdor, and G. J. Adema. 2001. Quantitative analysis of chemokine expression by dendritic cell subsets in vitro and in vivo. *J. Leukocyte Biol. 69:785*.
16. Rumsaeng, V., H. Vliagoftis, C. K. Oh, and D. D. Metcalfe. 1997. Lymphotactin gene expression in mast cells following Fcϵ receptor I aggregation. *J. Immunol. 158:1353*.
17. Boismenu, R., L. Feng, Y. Y. Xia, J. C. C. Chang, and W. L. Havran. 1996. Chemokines expression by intraepithelial γδ T cells: implications for the recruitment of inflammatory cells to damage epithelia. *J. Immunol. 157:985*.
18. Cipriani, B., G. Borsellino, F. Poccia, R. Placido, D. Tramonti, S. Bach, L. Battistini, and C. F. Brosnam. 2000. Activation of C-C β-chemokines in human peripheral blood γδ T cells by isopentenyl pyrophosphate and regulation by cytokines. *Chemokines. 95:39*.
19. Tikhonov, I., M. Kitabwalla, M. Wallace, M. Malkovsky, B. Volkman, and C. D. Pauza. 2001. Staphylococcal superantigens induce lymphotactin production by human $CD4^+$ and $CD8^+$ T cells. *Cytokine 16:73*.
20. Nagai, S., S. Hashimoto, T. Yamashita, N. Toyoda, T. Satoh, T. Suzuki, and K. Matsushima. 2001. Comprehensive gene expression profile of human activated T_h1- and T_h2-polarized cells. *Int. Immunol. 13:367*.
21. Zhang, S., N. W. Lukacs, V. A. Lawless, S. L. Kunkel, and M. H. Kaplan. 2000. Differential expression of chemokines in Th1 and Th2 cells is dependent on Stat6 but not Stat4. *J. Immunol. 165:10*.
22. Cerdan, C., E. Serfling, and D. Olive. 2000. The C-class chemokine, lymphotactin, impairs the induction of Th1-type lymphokines in human $CD4^+$ T cells. *Blood 96:420*.
23. Dorner, B. G., A. Scheffold, M. S. Rolph, M. B. Hűser, S. H. E. Kaufmann, A. Radbruch, I. E. A. Flesch, and R. A. Kroczek. 2002. MIP-1α, MIP-1β, RANTES, and ATAC/lymphotactin function together with IFN-γ as type 1 cytokines. *Proc. Natl. Acad. Sci. USA 99:6181*.
24. Kurt, R. A., M. Bauck, S. Harma, K. McCulloch, A. Baher, and W. J. Urba. 2001. Role of C chemokine lymphotactin in mediating recruitment of antigen-specific $CD62L^{lo}$ cells in vitro and in vivo. *Cell. Immunol. 209:83*.
25. Lillard, J. W., P. N. Boyaka, J. A. Hedrick, A. Zlotnik, and, J. R. McGhee. 1999. Lymphotactin acts as an innate mucosal adjuvant. *J. Immunol. 162:1959*.
26. Dilloo, D., K. Bacon, W. Holden, W. Zhong, S. Burdach, A. Zlotnik, and M. Brenner. 1996. Combined chemokine and cytokine gene transfer enhances antitumor immunity. *Nat. Med. 2:1090*.
27. Emtage, P. C. R., Y. Wan, M. Hitt, F. L. Graham, W. J. Muller, A. Zlotnik, and J. Gauldie. 1999. Adenoviral vectors expressing lymphotactin and interleukin-12 sinergize to facilitate tumor regression in murine breast cancer models. *Hum. Gene Ther. 10:697*.
28. Cao, X., W. Zhang, L. He, Z. Xie, S. Ma, Q. Tao, Y. Yu, H. Hamada, and J. Wang. 1998. Lymphotactin gene-modified bone marrow dendritic cells act as potent adjuvants for peptide delivery to induce specific antitumor immunity. *J. Immunol. 161:6238*.
29. Zhang, W., L. He, Z. Yuan, Z. Xie, J. Wang, H. Hamada, and X. Cao. 1999. Enhanced therapeutic efficacy of tumor RNA-pulsed dendritic cell after genetic modification with lymphotactin. *Hum. Gene Ther. 10:1151*.
30. Silvestri, B., F. Calderazzo, V. Coppola, A. Rosato, S. Iacobelli, C. Natoli, A. Ullrich, I. Sures, M. Azam, C. Brakebush, et al. 1998. Differential effect on TCR:CD3 stimulation of a 90kD glycoprotein (gp90/Mac-2BP), a member of the scavenger receptor cysteine-rich domain protein family. *Clin. Exp. Immunol. 113:394*.
31. Coppola, V., A. Veronesi, S. Indraccolo, F. Calderazzo, M. Mion, S. Minuzzo, G. Esposito, D. Mauro, B. Silvestri, P. Gallo, et al. 1998. Lymphoproliferative disease in human peripheral blood mononuclear cell-injected SCID mice. IV. Differential activation of human Th-1 and Th-2 lymphocytes and influence of the atopic status on lymphoma development. *J. Immunol. 160:2514*.
32. Indraccolo, S., S. Minuzzo, R. Zamarchi, F. Calderazzo, E. Piovan, and A. Amadori. 2002. Alternatively spliced forms of Igα and Igβ prevent B cell receptor expression on the cell surface. *Eur. J. Immunol. 32:1530*.
33. Indraccolo, S., E. Gola, A. Rosato, W. Habeler, V. Tisato, V. Roni, G. Esposito, M. Morini, A. Albini, D. M. Noonan, et al. 2002. Differential effects of angiostatin, endostatin and interferon-α1 gene transfer on in vivo growth of human breast cancer cells. *Gene Ther. 9:867*.
34. Indraccolo, S., W. Habeler, V. Tisato, L. Stievano, E. Piovan, V. Tosello, G. Esposito, R. Wagner, K. Uberla, L. Chieco-Bianchi, et al. 2002. Gene transfer in ovarian cancer cells: a comparison between retroviral and lentiviral vectors. *Cancer Res. 62:6099*.
35. Zhan, Y., X. Song, and G. W. Zhou. 2001. Structural analysis of regulatory protein domains using GST-fusion proteins. *Gene 281:1*.
36. Amadori, A., R. Zamarchi, M. L. Veronese, M. Panozzo, A. Barelli, A. Borri, M. Sironi, F. Colotta, A. Mantovani, and L. Chieco-Bianchi. 1991. B cell activation during HIV-1 infection. II. Cell-to-cell interactions and cytokine requirement. *J. Immunol. 146:57*.
37. Amadori, A., R. Zamarchi, G. De Silvestro, G. Forza, G. Cavattoni, G. A. Danieli, M. Clementi, and L. Chieco-Bianchi. 1995. Genetic control of the CD4/CD8 T-cell ratio in humans. *Nat. Med. 1:1279*.
38. Schmitz, J. E., M. A. Forman, M. A. Lifton, O. Concepcion, K. A. Reinmann, C. S. Crumpacker, J. F. Daley, R. S. Gelman, and N. L. Levin. 1998. Expression of the $CD8\alpha\beta$-heterodimer on $CD8^+$ T lymphocytes in peripheral blood lymphocytes of human immunodeficiency virus$^-$ and human immunodeficiency virus$^+$ individuals. *Blood 92:198*.
39. Olive, D., and C. Cerdan. 1999. CD28 co-stimolation results in down-regulation of lymphotactin expression in human $CD4^+$ but not $CD8^+$ T cells via an IL-2-dependent mechanism. *Eur. J. Immunol. 29:2443*.
40. Indraccolo, S., M. Mion, R. Zamarchi, V. Coppola, F. Calderazzo, A. Amadori, and L. Chieco-Bianchi. 1995. A $CD3^+CD8^+$ T cell population lacking CD5 antigen expression is expanded in peripheral blood of human immunodeficiency virus-infected patients. *Clin. Immunol. Immunopathol. 77:253*.
41. Trejdosiewicz, L. K., C. J. Smart, D. J. Oakes, P. D. Howdle, G. Malizia, D. Campana, and A. W. Boylston. 1989. Expression of T-cell receptors TcR1 (γ/δ) and TcR2 (α/β) in the human intestinal mucosa. *Immunology 68:7*.
42. Bierer, B. E., Y. Nishimura, S. J. Burakoff, and B. R. Smith. 1988. Phenotypic and functional characterization of human cytolytic T cells lacking expression of CD5. *J. Clin. Invest. 81:1390*.
43. Moebius, U., G. Kober, A. L. Griscelli, T. Hercend, and S. C. Meuer. 1991. Expression of different CD8 isoforms on distinct human lymphocyte subpopulations. *Eur. J. Immunol. 21:1793*.
44. Norment, A. M., and D. R. Littman. 1988. A second subunit of CD8 is expressed in human T cells. *EMBO J. 7:3433*.
45. Azzam, H. S., A. Grinberg, K. Lui, H. Shen, E. W. Shores, and P. E. Love. 1998. CD5 expression is developmentally regulated by T cell receptor (TCR) signals and TCR avidity. *J. Exp. Med. 188:2301*.
46. Chan, S., C. Waltzinger, A. Tarakhovsky, C. Benoist, and D. Mathis. 1999. An influence of CD5 on the selection of CD4-lineage T cells. *Eur. J. Immunol. 29:2916*.
47. Zhou, X. Y., Y. Yashiro-Ohtani, K. Toyo-Oka, C. S. Park, X. G. Tai, T. Hamaoka, and H. Fujiwara. 2000. CD5 costimulation up-regulates the signaling of extracellular signal-regulated kinase activation in $CD4^+CD8^+$ thymocytes and supports their differentiation to the CD4 lineage. *J. Immunol. 164:1260*.
48. Yoshida, T., T. Imai, M. Kakizaki, M. Nishimura, S. Takagi, and O. Yoshie. 1998. Identification of a single C motif-1/lymphotactin receptor XCR1. *J. Biol. Chem. 273:16551*.
49. Cairns, C. M., J. R. Gordon, F. Li, M. E. Baca-Estrada, T. Moyana, and J. Xiang. 2001. Lymphotactin expression by engineered myeloma cells drives tumor regression: mediation by CD4 and CD8 T cells and neutrophils expressing XCR1 receptor. *J. Immunol. 167:57*.
50. Xia, D. J., W. P. Zhang, S. Zheng, J. Wang, J. P. Pan, Q. Wang, L. H. Zhang, H. Hamada, and X. Cao. 2002. Lymphotactin cotransfection enhances the therapeutic efficacy of dendritic cells genetically modified with melanoma antigen gp100. *Gene Ther. 9:592*.
51. Huang, H., F. Li, J. R. Gordon, and J. Xiang. 2002. Synergistic enhancement of antitumor immunity with adoptively transferred tumor-specific $CD4^+$ and $CD8^+$ T cells and intratumoral lymphotactin transgene expression. *Cancer Res. 62:2043*.
52. Middel, P., P. Thelen, S. Blaschke, F. Polzien, K. Reich, V. Blaschke, A. Wrede, K. Mathias-Hummel, B. Gunawan, and H.-J. Radzun. 2001. Expression of the T-cell chemoattractant chemokine lymphotactin in Crohn's disease. *Am. J. Pathol. 159:1751*.
53. Ou, Z. L., O. Hotta, Y. Natori, H. Sugai, Y. Taguma, and Y. Natori. 2002. Enhanced expression of C chemokine lymphotactin in IgA nephropathy. *Nephron 91:262*.
54. Wang, J.-D., N. Nonomura, S. Takahara, B.-S. Li, H. Azuma, N. Ichimaru, Y. Kokado, K. Matsumiya, T. Miki, S. Suzuki, et al. 1998. Lymphotactin: a key regulator of lymphocyte trafficking during acute graft rejection. *Immunology 95:56*.

55. Yun, J. J., M. P. Fischbein, H. Laks, M. C. Fischbein, M. L. Espejo, K. Ebrahimi, Y. Irie, J. Berliner, and A. Ardehali. 2000. Early and late chemokine production correlates with cellular recruitment in cardiac allograft vasculopathy. *Transplantation 69:2515*.
56. Ou, Z. L., Y. Natori, and Y. Natori. 2000. Transient and sequential expression of chemokine mRNA in glomeruli in puromycin aminonucleoside nephrosis. *Nephron 85:254*.
57. Cerdan, C., E. Devilard, and D. Olive. 2001. The C-class chemokine lymphotactin costimulates the apoptosis of human $CD4^+$ T cells. *Blood 97:2205*.
58. Cristillo, A. D., M. J. Macri, and B. E. Bierer. 2003. Differential chemokine expression profiles in human peripheral blood T lymphocytes: dependence on T-cell coreceptor and calcineurin signaling. *Blood 101:216*.
59. Hautamaa, D., R. Merica, Z. Cheng, and M. K. Jenkins. 1997. Murine lymphotactin: gene structure, post-translational modification and inhibition of expression by CD28 costimulation. *Cytokine 9:375*.
60. Bierer, B. E., S. J. Burakoff, and B. R. Smith. 1989. A large proportion of T lymphocytes lack CD5 expression after bone marrow transplantation. *Blood 73:1359*.
61. McKay, P. J., A. McLaren, L. M. Andrews, and N. P. Lucie. 1991. Recovery of $CD3^+$ and $CD5^-$ lymphocyte subpopulation after autologous bone marrow transplantation and chemotherapy. *J. Clin. Pathol. 44:259*.
62. Terry, L. A., J. P. DiSanto, T. N. Small, and N. Flomenberg. 1990. Differential expression and regulation of the human CD8α and CD8β chains. *Tissue Antigens 35:82*.
63. Baume, D. M., M. A. Caligiuri, T. J. Manley, J. F. Daley, and J. Ritz. 1990. Differential expression of CD8α and CD8β associated with MHC-restricted and non-MHC-restricted cytolytic effector cells. *Cell. Immunol. 131:352*.
64. Pantaleo, G., and A. S. Fauci. 1995. New concepts in the immunopathogenesis of HIV infection. *Annu. Rev. Immunol. 13:487*.
65. Muller, S., M. Jungo, P. Aichele, and C. Mueller. 1997. $CD5^-$ CD8 $\alpha\beta$ intestinal intraepithelial lymphocytes (IEL) are induced to express CD5 upon antigen-specific activation: $CD5^-$ and $CD5^+$ CD8 $\alpha\beta$ IEL do not represent separate T cell lineages. *Eur. J. Immunol. 27:1756*.
66. Bensussan, A., C. Rabian, V. Schiavon, D. Bengoufa, G. Leca, and L. Boumsell. 1993. Significant enlargement of a specific subset of $CD3^+CD8^+$ peripheral blood leukocytes mediating cytotoxic T-lymphocyte activity during human immunodeficiency virus infection. *Proc. Natl. Acad. Sci. USA 90:9427*.
67. Borthwick, N. J., M. Bofill, I. Hassan, P. Panayiotidis, G. Janossy, M. Salmon, and A. N. Akbar. 1996. Factors that influence activated $CD8^+$ T-cell apoptosis in patients with acute herpesvirus infections: loss of costimulatory molecules CD28, CD5 and CD6 but relative maintenance of Bax and Bcl-X expression. *Immunology 88:508*.
68. Shimojima, M., T. Miyazawa, M. Kohmoto, Y. Ikeda, Y. Nishimura, K. maeda, Y. Tohya, and T. Mikami. 1998. Expansion of CD8 $\alpha^+\beta^-$ cells in cats infected with feline immunodeficiency virus. *J. Gen. Virol. 79:91*.
69. McKay, P. J., B. Kyle, A. McLaren, M. A. McMillan, and N. P. Lucie. 1991. $CD5^-$ T lymphocytes in renal transplant recipients. *Clin. Lab. Haematol. 13:335*.